Statistical Mechanics
E0415

Fall 2022, lecture 8
Quantum phase transitions

... take home...

“I chose the paper "Splitting up entropy into vibrational and configurational contributions in bulk metallic glasses: A thermodynamic approach", because I know from the past that neurostuff can be very confusing and wanted to avoid that. The article discussed entropy of metallic glasses, i.e. amorphous metals…. The methods for studying it were computational as they utilized molecular dynamics… The system size was relatively small with only 4000 atoms, but still the results matched the experiments well in case of $Cu_{50}Zr_{50}$. The main results were that the entropy originating from the number of different configurations, configurational entropy, and vibrational part. The authors found that the configurational part was constant with respect to temperature.”

”The glass with aluminium has better glass forming abilityin the real world suggesting that studying the configurational entropies could help understand glass forming ability of bulk metallic glasses.”

”I chose this study as I am taking a course in neuroscience this semester and I was interested in linking these two domains. … This article wants to analyze the distribution of entropy in the brain and its evolution via a brain scanning method with fMRI. The hypothesis made was that the entropy has a determinate structure and fluctuations according to the different regions of the brain, and this discrimination is determined by neuronal dynamics. … The study found clear hierarchical BEN clusters and significant contrast between grey and white matter. In conclusion, BEN provided a clear mapping of brain activity (at resting state), which could become an interesting index to further investigate mental disorders or dysfunctionings”

…. On the papers ….

"Brain Entropy Mapping Using fMRI by Ze Wang et. al. explores the possibility to use for fMRI to measure brain entropy or BEN. This information could be used for determining brain status or to detect anomalous brain activity since human brain has normally approximately constant entropy. Also, background and nonliving objects have higher entropy in comparison which allows for distinction of living tissue.

Structural MRI, resting state fMRI and fMRI under sensorimotor action were measured from 16 young and healthy subjects twice and two months apart. BEN mapping was computed using sample entropy for both fMRI measurements and clear decrease in entropy was detected when sensorimotor tasks were performed.

A mean BEN mapping was also calculated from a dataset containing resting state fMRI measurements from 1049 subjects, which shows a clear distinction between neocortex, white matter, and subcortical gray matter structures. The data was used to divide the brain into 8 distinctive BEN clusters. The results indicated that fMRI can be robustly used for brain activity mapping using sample entropy“

"The article discusses that the total entropy in bulk metallic glasses originates from vibrational and configurational contributions. The configurational contribtuion comes from the exploration of different basins, while the vibrational part is result of intrabasin thermal motion. This splitting is possible thanks to the description known as potential-energy landscape (PEL), stating that below glass transition temperature (Tg) the liquid (glass) is frozen in a single configuration, and unable to explore different configurations. The work done in the article was computational, and simulations were used to explore the entropies of one binary and one ternary bulk metallic glasses. If I understood correctly, directly calculating the contribution of configurational entropy is quite difficult. However, the vibrational contribution could be calculated more easily, as well as the total entropy of the system. As long as the T < Tg, the total entropy of the system is directly just the entropy of the glass, and thus subtracting the vibrational contribution gives the configurational contribution. The results obtained were relatively similar to the ones obtained recently using experimental methods."

Outline of lecture

1) Idea of a QPT
2) Quantum Transverse Ising model
3) Phase diagrams
4) Scaling hypothesis: classical vs. quantum
5) Classical-quantum mapping
6) Quantum annealing
7) Kibble-Zurek mechanism

Quantum Ising

transverse-field quantum Ising model: $\langle ij \rangle$: nearest neighbours

$$\mathcal{H} = -J \sum_{\langle ij \rangle} \hat{\sigma}_i^z \hat{\sigma}_j^z - Jg \sum_i \hat{\sigma}_i^x$$

- each site i has spin-$\frac{1}{2}$ d.o.f.
- $\hat{\sigma}_i^\mu$: operators obeying $[\hat{\sigma}_i^\mu, \hat{\sigma}_j^\nu] = -2i\epsilon_{\mu\nu\rho}\hat{\sigma}_i^\rho \delta_{ij}$
- in $\hat{\sigma}^z$ basis, $|\uparrow\rangle_i$, $|\downarrow\rangle_i$, $\hat{\sigma}_i^\mu |s\rangle_i = (\boldsymbol{\sigma}^\mu)_{ss'} |s'\rangle_i$

$s, s' \in \{+1, -1\}$

$\boldsymbol{\sigma}^\mu$: Pauli matrix

$$\hat{\sigma}_i^z |\uparrow\rangle_i = +|\uparrow\rangle_i \qquad \hat{\sigma}_i^z |\downarrow\rangle_i = -|\downarrow\rangle_i$$
$$\hat{\sigma}_i^x |\uparrow\rangle_i = |\downarrow\rangle_i \qquad \hat{\sigma}_i^x |\downarrow\rangle_i = |\uparrow\rangle_i$$

Quantum Ising model has symmetry under spin-flip operator $U = \prod_i \hat{\sigma}_i^x$

i.e., $[\mathcal{H}, U] = 0$

$$\hat{\sigma}_i^z \xrightarrow{U} U\hat{\sigma}_i^z U^{-1} = -\hat{\sigma}_i^z$$
$$\hat{\sigma}_i^z \hat{\sigma}_j^z \xrightarrow{U} \hat{\sigma}_i^z \hat{\sigma}_j^z$$
$$\hat{\sigma}_i^x \xrightarrow{U} \hat{\sigma}_i^x$$

Paramagnet

$$\mathcal{H} = -J \sum_{\langle ij \rangle} \hat{\sigma}_i^z \hat{\sigma}_j^z - Jg \sum_i \hat{\sigma}_i^x$$

$$\left.\begin{array}{l} \hat{\sigma}_i^x |\uparrow\rangle_i = |\downarrow\rangle_i \\ \hat{\sigma}_i^x |\downarrow\rangle_i = |\uparrow\rangle_i \end{array}\right\} \quad \hat{\sigma}_i^x |\rightarrow\rangle_i = +|\rightarrow\rangle_i \text{ where } |\rightarrow\rangle = \frac{1}{\sqrt{2}}(|\uparrow\rangle + |\downarrow\rangle)$$

For $g \to +\infty$, $|\text{g.s.}\rangle = \prod_i |\rightarrow\rangle_i$

spins align with applied field: "quantum paramagnet"

g.s. is symmetric under spin flip: $U|\text{g.s.}\rangle = |\text{g.s.}\rangle$

$\langle \text{g.s.}|\hat{\sigma}_i^z|\text{g.s.}\rangle = 0$ $\qquad U = \prod_i \hat{\sigma}_i^x$

product state, so no correlations: $\langle \text{g.s.}|\hat{\sigma}_i^z \hat{\sigma}_j^z|\text{g.s.}\rangle = \delta_{ij}$

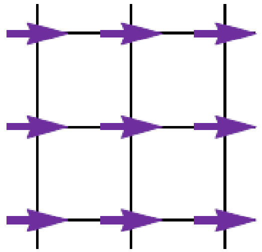

For large finite g, $|\text{g.s.}\rangle = \prod_i |\rightarrow\rangle_i$ + perturbative corrections in $1/g$

correlations $\langle \text{g.s.}|\hat{\sigma}_i^z \hat{\sigma}_j^z|\text{g.s.}\rangle \sim e^{-|x_i - x_j|/\xi}$ with $\xi \to 0$ for $g \to \infty$

"kinetic energy (i.e., off-diagonal term) wins"

("kinetic"/"potential" depends on choice of basis)

Ferromagnet

$$\mathcal{H} = -J \sum_{\langle ij \rangle} \hat{\sigma}_i^z \hat{\sigma}_j^z - Jg \sum_i \hat{\sigma}_i^x$$

For $g = 0$, two degenerate ground states: $|\Uparrow\rangle = \prod_i |\uparrow\rangle_i$ and $|\Downarrow\rangle = \prod_i |\downarrow\rangle_i$

spins align with each other: ferromagnet

both states break spin-flip symmetry ($U|\Uparrow\rangle = |\Downarrow\rangle$)

$\langle \text{g.s.}|\hat{\sigma}_i^z|\text{g.s.}\rangle = 1$

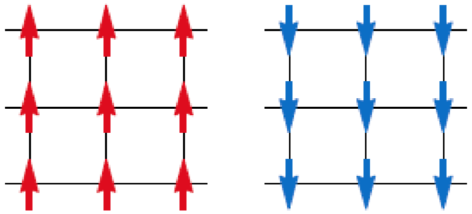

product state: $\langle \text{g.s.}|\hat{\sigma}_i^z \hat{\sigma}_j^z|\text{g.s.}\rangle = \langle \text{g.s.}|\hat{\sigma}_i^z|\text{g.s.}\rangle \langle \text{g.s.}|\hat{\sigma}_j^z|\text{g.s.}\rangle = 1$

For $g = 0^+$, superpositions $|\Uparrow\rangle \pm |\Downarrow\rangle$ are e'states, but splitting $\to 0$ as $N \to \infty$

$N = \infty$: macroscopic superpos'ns unstable; take $|\Uparrow\rangle$, $|\Downarrow\rangle$ as degenerate g.s.

for small g and $N = \infty$, $|\text{g.s.}_+\rangle = \prod_i |\uparrow\rangle_i$ + perturbative corrections in g
$|\text{g.s.}_-\rangle = \prod_i |\downarrow\rangle_i$ + perturbative corrections in g

"potential energy (i.e., diagonal term) wins"

Partititon function

at temperature $T = 1/\beta$, partition function

$$Z = \mathrm{Tr}\, e^{-\beta\mathcal{H}}$$

$$= \sum_{s} \langle s | e^{-\beta\mathcal{H}} | s \rangle$$

for any (orthonormal) basis $\{|s\rangle\}$

split operator $e^{-\beta\mathcal{H}}$ into M pieces $e^{-a\mathcal{H}}$ with $Ma = \beta$:

$$Z = \sum_{s_0} \langle s_0 | \underbrace{e^{-a\mathcal{H}} e^{-a\mathcal{H}} \cdots e^{-a\mathcal{H}}}_{M} | s_0 \rangle$$

$$\sum_{s} |s\rangle\langle s| = 1$$

$$= \sum_{s_0, s_1, \ldots, s_{M-1}} \langle s_0 | e^{-a\mathcal{H}} | s_1 \rangle \langle s_1 | e^{-a\mathcal{H}} | s_2 \rangle \langle s_2 | \cdots | s_{M-1} \rangle \langle s_{M-1} | e^{-a\mathcal{H}} | s_0 \rangle$$

$e^{-a\mathcal{H}}$: evolution by "imaginary time" $t = -ia$

(real-time evolution operator $e^{-i\mathcal{H}t}$)

$\sum_{s_0, s_1, \ldots, s_{M-1}}$: sum over trajectories

"path integral" representation of Z

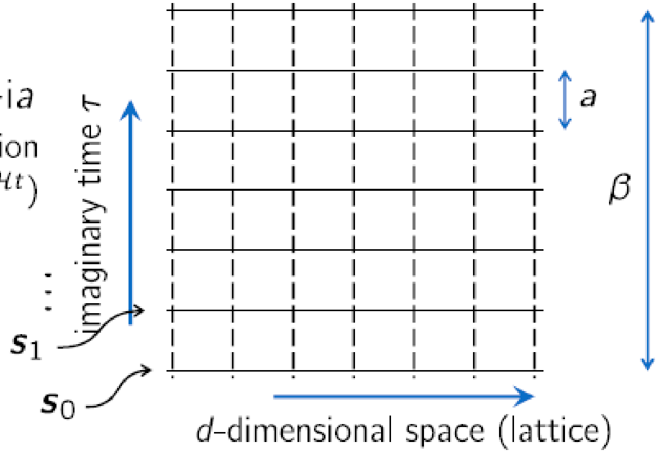

Quantum model to classical mapping

$$Z = \sum_{s_0, s_1, \ldots, s_{M-1}} \langle s_0 | e^{-a\mathcal{H}} | s_1 \rangle \langle s_1 | e^{-a\mathcal{H}} | s_2 \rangle \langle s_2 | \cdots | s_{M-1} \rangle \langle s_{M-1} | e^{-a\mathcal{H}} | s_0 \rangle$$

choose basis states $|\boldsymbol{s}\rangle$ corresponding
to classical configurations $\boldsymbol{s}$

define $\mathcal{E}(\boldsymbol{s}, \boldsymbol{s}') = -\log \langle \boldsymbol{s} | e^{-a\mathcal{H}} | \boldsymbol{s}' \rangle = [\mathcal{E}(\boldsymbol{s}', \boldsymbol{s})]^*$

$$Z = \sum_{s_0, s_1, \ldots, s_{M-1}} e^{-\sum_{i=0}^{M-1} \mathcal{E}(s_i, s_{i+1})}$$

where $\boldsymbol{s}_M \equiv \boldsymbol{s}_0$ (periodicity in τ)

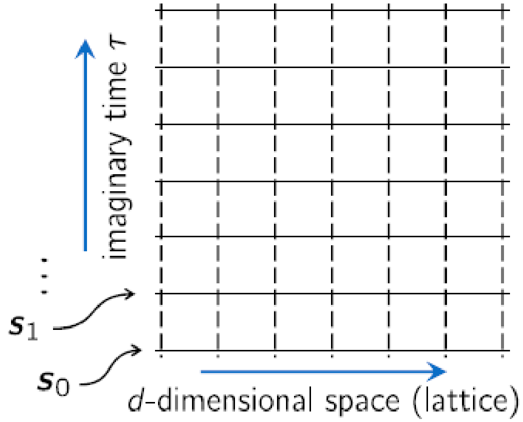

cf. classical statistical system with reduced Hamiltonian E_{cl}
on $(d+1)$-dimensional lattice (with p.b.c.)

$$E_{\mathrm{cl}} = \sum_i [E_1(\boldsymbol{s}_i) + E_2(\boldsymbol{s}_i, \boldsymbol{s}_{i+1})]$$

E_1: layer configuration energy
E_2: interaction between adjacent layers

$$= \sum_i \left\{ \frac{1}{2} [E_1(\boldsymbol{s}_i) + E_1(\boldsymbol{s}_{i+1})] + E_2(\boldsymbol{s}_i, \boldsymbol{s}_{i+1}) \right\} = \sum_{i=0}^{M-1} E(\boldsymbol{s}_i, \boldsymbol{s}_{i+1})$$

if $\mathcal{E}(\boldsymbol{s}, \boldsymbol{s}')$ is real, interpret Z as partition f'n for classical $(d+1)$-dimensional system

Summary

quantum	classical
imaginary time τ	extra spatial dimension τ
inverse temperature $\beta = \frac{1}{T}$	system size L_τ in τ direction
imaginary-time evolution $e^{-a\mathcal{H}}$	Boltzmann weight (transfer matrix) $e^{-\mathcal{E}(s,s')} = \langle \boldsymbol{s} \vert e^{-a\mathcal{H}} \vert \boldsymbol{s}' \rangle$
sum over trajectories ("path integral")	sum over configurations (canonical ensemble)
quantum critical phenomena at $T = 0$ in d dimensions	classical critical phenomena in $d + 1$ dimensions

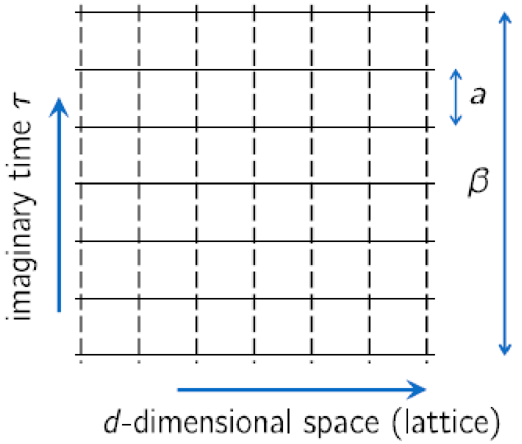

- at zero temperature, $\beta = 1/T = \infty$: imaginary-time direction is infinite
- n.b., distinct from relationship between classical stochastic dynamics (in d dimensions) and quantum mechanics (in d dimensions)

Ising again

transverse–field quantum Ising model: $\mathcal{H} = -J \sum_{\langle ij \rangle} \hat{\sigma}_i^z \hat{\sigma}_j^z - Jg \sum_i \hat{\sigma}_i^x$

define $\mathcal{E}(\boldsymbol{s}, \boldsymbol{s}') = -\log \langle \boldsymbol{s} | \mathrm{e}^{-a\mathcal{H}} | \boldsymbol{s}' \rangle$

$$Z = \sum_{\boldsymbol{s}_0, \boldsymbol{s}_1, \ldots, \boldsymbol{s}_{M-1}} \mathrm{e}^{-\sum_{i=0}^{M-1} \mathcal{E}(\boldsymbol{s}_i, \boldsymbol{s}_{i+1})}$$

use $\hat{\sigma}_i^z$ basis, $|\uparrow\rangle_i$, $|\downarrow\rangle_i$:

$$|\boldsymbol{s}\rangle = |\{s_1, s_2, \ldots s_N\}\rangle = \prod_i^N |s_i\rangle_i,$$

for sufficiently small a, use $\mathrm{e}^{a(A+B)} = \mathrm{e}^{aA}\mathrm{e}^{aB}[1 + \mathcal{O}(a)]$

$$\begin{aligned}
\langle \boldsymbol{s} | \mathrm{e}^{-a\mathcal{H}} | \boldsymbol{s}' \rangle &\approx \langle \boldsymbol{s} | \mathrm{e}^{aJg \sum_i \hat{\sigma}_i^x} \mathrm{e}^{aJ \sum_{\langle ij \rangle} \hat{\sigma}_i^z \hat{\sigma}_j^z} | \boldsymbol{s}' \rangle \\
&= \langle \boldsymbol{s} | \mathrm{e}^{aJg \sum_i \hat{\sigma}_i^x} | \boldsymbol{s}' \rangle \, \mathrm{e}^{aJ \sum_{\langle ij \rangle} s_i' s_j'} \\
&= \mathrm{e}^{aJ \sum_{\langle ij \rangle} s_i' s_j'} \prod_i \langle s_i | \mathrm{e}^{aJg\hat{\sigma}^x} | s_i' \rangle \\
&= [A(aJg)]^N \mathrm{e}^{aJ \sum_{\langle ij \rangle} s_i' s_j' + B(aJg) \sum_i s_i s_i'}
\end{aligned}$$

$$\langle s | \mathrm{e}^{\alpha\hat{\sigma}^x} | s' \rangle = A(\alpha) \mathrm{e}^{B(\alpha) s s'}$$

$$B(\alpha) = -\tfrac{1}{2} \log \tanh \alpha$$

$$\mathcal{E}(\boldsymbol{s}, \boldsymbol{s}') = -aJ \sum_{\langle ii \rangle} s_i' s_j' - B(aJg) \sum_i s_i s_i' + \text{const}$$

Ising II

transverse-field quantum Ising model: $\mathcal{H} = -J \sum_{\langle ij \rangle} \hat{\sigma}_i^z \hat{\sigma}_j^z - Jg \sum_i \hat{\sigma}_i^x$

$$Z = \sum_{\mathbf{s}_0, \mathbf{s}_1, \ldots, \mathbf{s}_{M-1}} \mathrm{e}^{-\sum_{i=0}^{M-1} \mathcal{E}(\mathbf{s}_i, \mathbf{s}_{i+1})}$$

For $a \to 0$, $\quad B(\alpha) = -\frac{1}{2} \log \tanh \alpha$

$$\mathcal{E}(\mathbf{s}, \mathbf{s}') = -aJ \sum_{\langle ij \rangle} s_i' s_j' - B(aJg) \sum_i s_i s_i'$$

layer configuration energy

interaction between adjacent layers

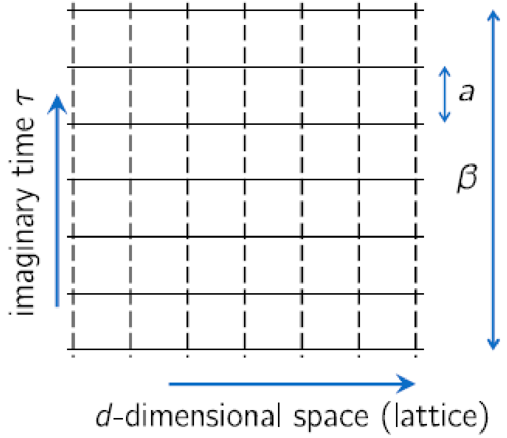

- Transverse-field Ising model in d dimensions maps to highly anisotropic ($a \to 0$) classical Ising model in $d + 1$ dimensions
- By universality, quantum Ising model has identical critical properties to isotropic classical Ising model in $d + 1$ dimensions

Ising chain

transverse-field quantum Ising model in 1D:

$$\mathcal{H} = -J \sum_i \left[\hat{\sigma}_i^z \hat{\sigma}_{i+1}^z + g\hat{\sigma}_i^x\right]$$

(related to 2D classical Ising model, so ordering transition at g_c)

for $g = \infty$, $|\text{g.s.}\rangle = \prod_i |{\rightarrow}\rangle_i$

excited states have flipped spins

for large g, use perturbation theory, with $\delta\mathcal{H} = \sum_i \hat{\sigma}_i^z \hat{\sigma}_{i+1}^z$

$\delta\mathcal{H}$ creates flipped spins in pairs & hops them between sites

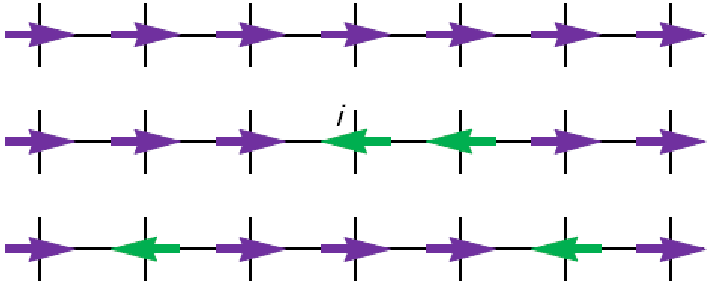

$$|{\rightarrow}\rangle = \frac{1}{\sqrt{2}}\left(|{\uparrow}\rangle + |{\downarrow}\rangle\right) \qquad \hat{\sigma}^z|{\rightarrow}\rangle = |{\leftarrow}\rangle$$

$$|{\leftarrow}\rangle = \frac{1}{\sqrt{2}}\left(|{\uparrow}\rangle - |{\downarrow}\rangle\right) \qquad \hat{\sigma}^z|{\leftarrow}\rangle = |{\rightarrow}\rangle$$

so treat flipped spins as particles

Use a transformation....

Treat flipped spins as particles

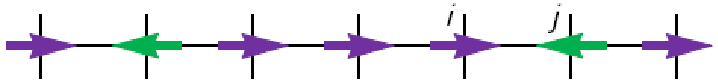

either:

- as bosons—but then need interactions to forbid two flipped spins on one site

$\hat{\sigma}_i^x = 1 - 2n_i \qquad n_i = 0$

$\hat{\sigma}_i^z = b_i + b_i^\dagger \qquad n_j = 1$

- as fermions—double occupation automatically forbidden, *but* fermion operators anticommute on different sites:

$$\{c_i, c_j^\dagger\} = \delta_{ij}$$

$$\{c_i, c_j\} = \{c_i^\dagger, c_j^\dagger\} = \delta_{ij}$$

$$[\hat{\sigma}_i^\mu, \hat{\sigma}_j^\nu] = -2i\epsilon_{\mu\nu\rho}\hat{\sigma}_i^\rho\delta_{ij}$$

Jordan–Wigner transformation (in 1D): add a string of minus signs

$$\hat{\sigma}_i^x = 1 - 2n_i \qquad n_j = c_j^\dagger c_j$$

$$\hat{\sigma}_i^z = -(c_i + c_i^\dagger)\prod_{j<i}(1 - 2n_j)$$

including this string, $[\hat{\sigma}_i^x, \hat{\sigma}_j^z] = 0$ for $i \neq j$, as required

… diagonalize… exact spectrum.

transverse-field quantum Ising model in 1D: $\mathcal{H} = -J\sum_i \left[\hat{\sigma}_i^z \hat{\sigma}_{i+1}^z + g\hat{\sigma}_i^x\right]$

JW transformation: $\hat{\sigma}_i^x = 1 - 2n_i \qquad n_j = c_j^\dagger c_j$

$$\hat{\sigma}_i^z = -(c_i + c_i^\dagger)\prod_{j<i}(1-2n_j)$$

$$\hat{\sigma}_i^z \hat{\sigma}_{i+1}^z = (c_i + c_i^\dagger)(c_{i+1} + c_{i+1}^\dagger)\prod_{j<i}(1-2n_j)\prod_{j'<i+1}(1-2n_{j'})$$

$$= (c_i + c_i^\dagger)(c_{i+1} + c_{i+1}^\dagger)(1-2n_i) \qquad \{c_i, c_j^\dagger\} = \delta_{ij}$$

$$= (-c_i + c_i^\dagger)(c_{i+1} + c_{i+1}^\dagger) \qquad \{c_i, c_j\} = \{c_i^\dagger, c_j^\dagger\} = \delta_{ij}$$

result: quadratic Hamiltonian in terms of fermion operators

$$\mathcal{H} = -J\sum_i \left(c_i^\dagger c_{i+1} + c_{i+1}^\dagger c_i + c_i^\dagger c_{i+1}^\dagger + c_{i+1}c_i - 2gc_i^\dagger c_i + g\right)$$

(see practice problems)

diagonalize with FT and unitary transformation: $c_k = u_k\gamma_k + iv_k\gamma_{-k}^\dagger \qquad \{\gamma_k, \gamma_k^\dagger\} = \delta_{k,k'}$

$$\mathcal{H} = \sum_k \varepsilon_k(\gamma_k^\dagger\gamma_k - \tfrac{1}{2})$$

ground state $|\text{g.s.}\rangle$: $\gamma_k|\text{g.s.}\rangle = 0$ (all k)

$$\varepsilon_k = 2J\sqrt{1 + g^2 - 2g\cos k}$$

gap $\Delta = E_1 - E_{\text{g.s.}} = \varepsilon_0 = 2J|1-g|$

Chain: QPT

$$\mathcal{H} = -J \sum_{\langle ij \rangle} \hat{\sigma}_i^z \hat{\sigma}_j^z - Jg \sum_i \hat{\sigma}_i^x = \sum_k \varepsilon_k (\gamma_k^\dagger \gamma_k - \tfrac{1}{2})$$

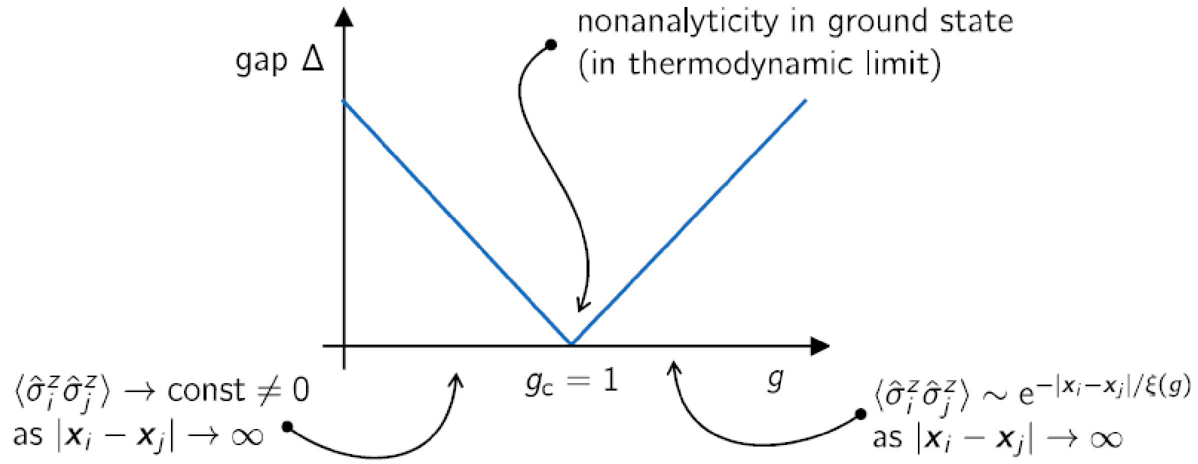

$$\varepsilon_k = 2J\sqrt{1 + g^2 - 2g\cos k}$$

$$\Delta = 2J|1-g| \sim |g - g_c|^{z\nu}$$

critical exponent $z\nu = 1$

Sachdev (1999/2011)

Quantum annealing

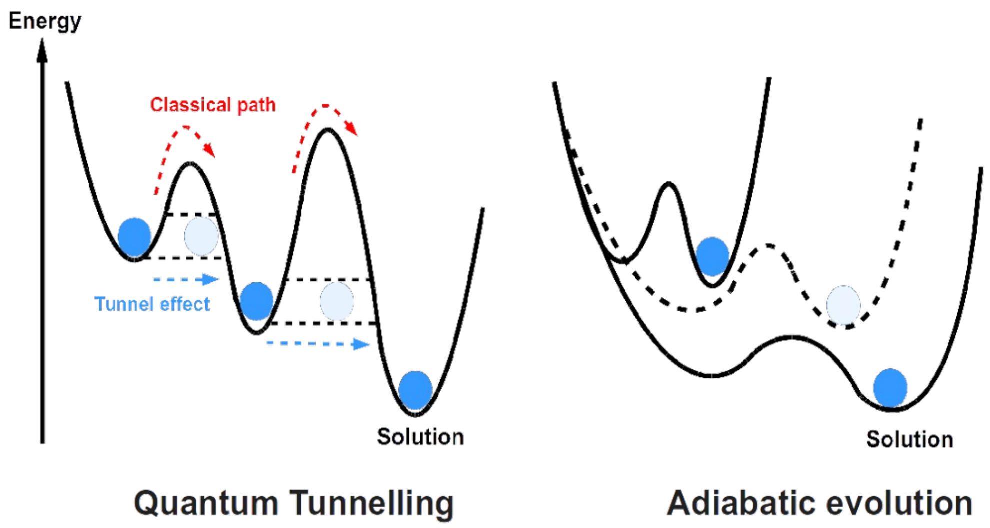

Idea: take a classical Hamiltonian (energy function). Instead of doing things at finite T and lowering it (Simulated Annealing)… Glauber dynamics with a decreasing T.

Do the quantum version with decreasing quantum effects.

Tunneling through barriers.

Kibble-Zurek

Approach a 2nd order phase transition at a (fixed) finite rate. Eg. The Ising transition.

At some point, the correlation time / relaxation timescale becomes so large, that the system no longer relaxes ("adiabatically") or is able to follow the change.

Consequence: topological defects are created. The density depends on the correlation scale (length) and dimension ("coherent volumes").

Lots of applications…

Physics depends on the rate of approach (velocity).

Kibble-Zurek II

Kibble-Zurek mechanism in colloidal monolayers

Sven Deutschländer,[1] Patrick Dillmann,[1] Georg Maret,[1] and Peter Keim[1,*]

PNAS 2015

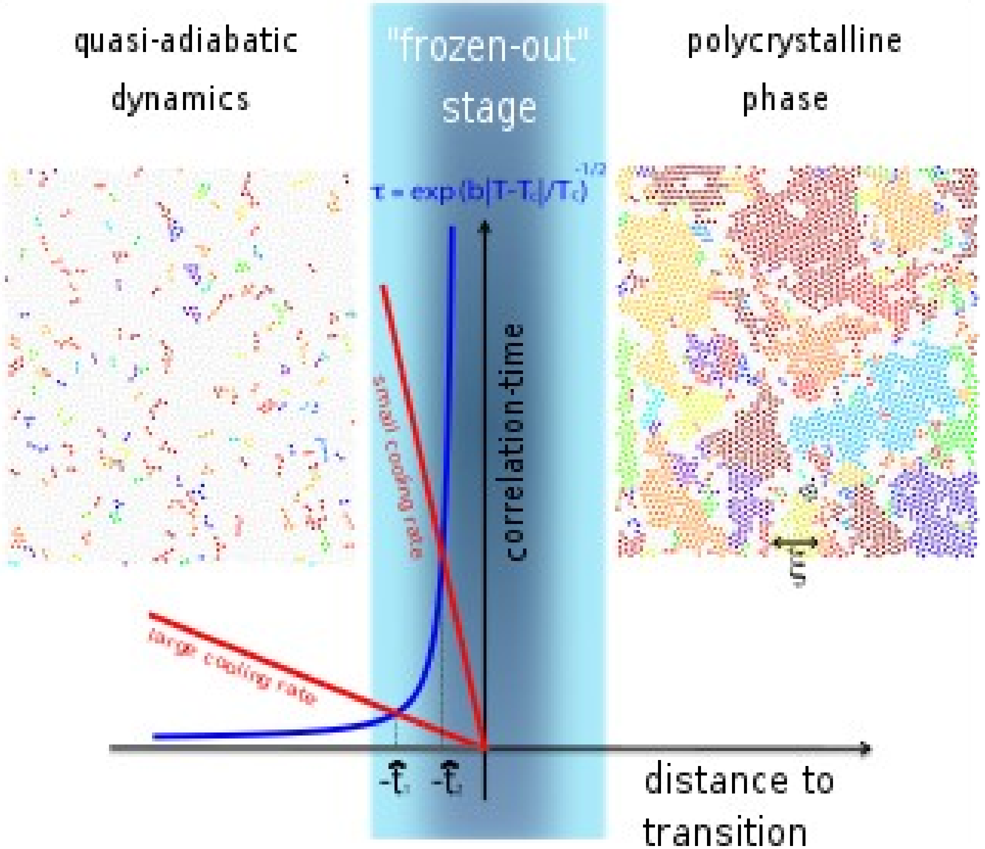

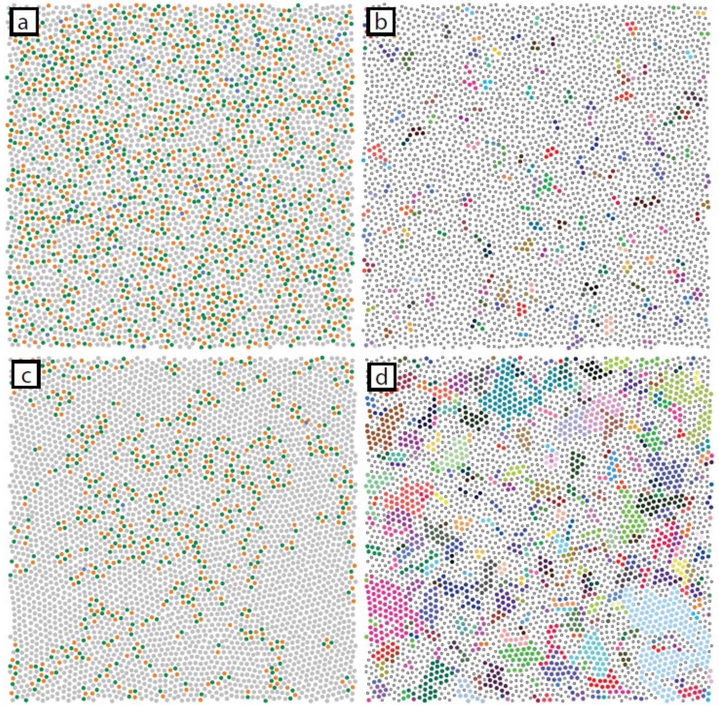

FIG. 5. Snapshot sections of the colloidal ensemble ($992 \times 960\ \mu m^2$, ≈ 4000 particles) illustrating the defect (a,c) and domain configurations (b,d) at the freeze out temperature $\hat{\Gamma}$ for the fastest (a,b: $\dot{\Gamma} = 0.0326$ 1/s, $\hat{\Gamma} \approx 30.3$) and slowest cooling rate (c,d: $\dot{\Gamma} = 0.000042$ 1/s, $\hat{\Gamma} \approx 66.8$). The defects are marked as follows: Particles with five nearest neighbors are colored red, seven nearest neighbors green and other defects blue. Sixfold coordinated particles are colored grey. Different symmetry broken domains are colored individually and high symmetry particles are displayed by smaller circles.

Quantum take-home

The classic reference for this stuff is by Subir Sachdeev (Quantum Phase Transitions) but we utilize here two sets of lecture notes that exploit it. The first set is from Warwick

https://warwick.ac.uk/fac/sci/physics/mpags/modules/theory/cqpt/lectures9-10.pdf

And if you want another viewpoint, with partly more detail, check lectures 5 and 6 from Dresden (Lukas Jansssen), https://tu-dresden.de/mn/physik/itp/tfp/studium/lehre/ss18/qpt_ss18

For the applications, we have quantum annealing and the Kibble-Zurek mechanism. The take home is now like this: check those notes so that you recall the main points of QPT. Then pick either a topic on quantum annealing (including the D-Wave simulator), in other words

https://www.nature.com/articles/s41598-019-49172-3

... or if you want to have more insight on the Kibble-Zurek, you should take

https://www.nature.com/articles/s41586-019-1070-1

And your task is like the previous time "2+8" sentences on the selection and main points.